ISSN 1027-4510, Journal of Surface Investigation: X-ray, Synchrotron and Neutron Techniques, 2022, Vol. 16, No. 1, pp. 7–12. © Pleiades Publishing, Ltd., 2022.
Russian Text © The Author(s), 2022, published in Poverkhnost', 2022, No. 1, pp. 10–17.

Release of TRITC-Dextran from Composite Microcapsules under the Influence of a Low-Frequency Alternating Magnetic Field

A. V. Mikheev[a, b, *], I. A. Burmistrov[b], V. B. Zaitsev[a], V. V. Artemov[b], D. N. Khmelenin[b], S. S. Starchikov[b], M. M. Veselov[a], N. L. Klyachko[a], T. V. Bukreeva[b, c], and D. B. Trushina[b, d]

[a] *Moscow State University, Moscow, 119991 Russia*
[b] *Federal Research Center "Crystallography and Photonics," Russian Academy of Sciences, Moscow, 119333 Russia*
[c] *National Research Center "Kurchatov Institute," Moscow, 123182 Russia*
[d] *Sechenov University, Moscow, 119991 Russia*
**e-mail: mikheev.av16@physics.msu.ru*

Received May 25, 2021; revised June 20, 2021; accepted June 25, 2021

Abstract—Composite microcapsules based on polyelectrolytes and nanoparticles of iron oxides are synthesized, and the release of encapsulated high-molecular dextran under the influence of a low-frequency alternating magnetic field due to the magnetomechanical actuation of nanoparticles in a polymer shell is investigated. As a result of the chemical condensation of ferrous and ferric iron, single-domain magnetic spherical Fe_3O_4 nanoparticles are synthesized and characterized by transmission electron microscopy, dynamic light scattering, powder X-ray diffraction, and Mössbauer spectroscopy. Polyelectrolyte microcapsules from polyallylamine hydrochloride and sodium polystyrene sulfonate are modified with magnetic nanoparticles due to electrostatic adsorption on an oppositely charged polyelectrolyte layer. Dextran, labeled with tetramethyl rhodamine-5-isothiocyanate (TRITC-dextran), is used as the model substance for encapsulation; it is incorporated into $CaCO_3$ particles (soluble cores for the formation of capsules) by coprecipitation. The capsule samples are examined by scanning electron microscopy, dynamic light scattering, and fluorescence confocal microscopy. The capsules are exposed to an alternating magnetic field with an amplitude of 100 mT and frequencies of 30–110 Hz. The content of labeled dextran in the shell of the microcapsules and the supernatant is determined using fluorimetry and fluorescence confocal microscopy. The duration of exposure and the frequency of the magnetic field, at which the maximum release of dextran from composite capsules is achieved, are established. Exposure to a low-frequency alternating magnetic field can lead to significant deformation of the shell of polyelectrolyte microcapsules modified with magnetic nanoparticles and successful release of the encapsulated substance.

Keywords: layer-by-layer adsorption, calcium carbonate, polyelectrolyte microcapsules, single-domain magnetic nanoparticles, iron oxide, Brownian relaxation of the magnetic moment, magnetomechanical actuation, low-frequency alternating magnetic field

DOI: 10.1134/S1027451021060355

INTRODUCTION

At present, the development of encapsulation systems and the targeted delivery of different substances followed by the controlled and/or gradual release of an encapsulated substance is an important issue in medicine and biotechnology. There are various delivery systems, including liposomes [1], micelles [2], vesicles [3], but polyelectrolyte microcapsules [4], developed by E. Donath and G. B. Sukhorukov in 1998, are of specific interest. Such capsules are being intensively studied and applied for the encapsulation and delivery of some biologically active substances in vitro and in vivo [5, 6]; in particular, polyelectrolyte capsules are promising for vaccine delivery [7–9].

Substances are released from polyelectrolyte capsules due to diffusion; the diffusion rate depends on the characteristics of encapsulated molecules (for example, on the size of the molecule), the properties of the polymer complex forming microcapsules, the shell thickness, and some other parameters [10]. The controlled release of substances implies the use of triggers that initiate this process in composite microcapsules having shells functionalized with suitable molecules and/or nanoparticles. The following triggers can be used: the action of enzymes [11], an ultrasonic field [12, 13], microwave field [14], and laser radiation [15, 16]. An alternating magnetic field can affect the release of the content of composite capsules and their integrity [17, 18].

When magnetic nanoparticles are placed in an alternating magnetic field, chaotically oriented magnetic moments will turn in one direction. Depending

on the characteristics of the nanoparticles and magnetic-field parameters, two types of magnetic-moment relaxation are distinguished. In the first case, the magnetic moment rotates, and the nanoparticle remains stationary which is Néel relaxation leading to heating of the environment. The phenomenon of magnetic hyperthermia is based on Néel relaxation [18, 19]. However, an increase in temperature can affect both thermosensitive biologically effective particles and surrounding tissues.

Particular attention should be paid to using a non-heating low-frequency magnetic field (frequency 1 to 1000 Hz) that has greater penetrability into tissues, ease of dosing and control, greater locality, and safety compared to a heating magnetic field [20]. When the magnetic moment is motionless relative to the nanoparticle in a low-frequency magnetic field, and the nanoparticle rotates in magnetic fields, it is called Brownian relaxation. This process does not lead to noticeable heat release, and the main channel of energy dissipation is deformation-mechanical (magnetomechanical activation) [17, 21, 22]. To date, only a few works have been devoted to the effect of low-frequency alternating magnetic fields on polyelectrolyte microcapsules [17, 22].

This work aims to synthesize composite microcapsules based on biodegradable polyelectrolytes and Fe_3O_4 nanoparticles and to study the released encapsulated molecules of high molecular weight dextran under the effect of a low-frequency alternating magnetic field due to the magnetomechanical activation of nanoparticles in a polymer shell.

EXPERIMENTAL

Materials

The following analytical-grade chemicals were used without additional purification: calcium chloride dihydrate $CaCl_2 \cdot 2H_2O$ (Acros Organics, USA), anhydrous sodium carbonate Na_2CO_3 (ITW Reagents, USA), sodium chloride NaCl, polysterene sodium sulfonate (PSS) (M_w = 70 kDa), polyallylamine hydrochloride (PAH) (M_w = 50 kDa)), TRITC-dextran (M_w = 65–85 kDa), iron chloride tetrahydrate $FeCl_2 \cdot 4H_2O$, ferric chloride hexahydrate $FeCl_3 \cdot 6H_2O$, disodium salt dihydrate ethylenediaminetetraacetic acid (EDTA) produced by Sigma Aldrich, Germany. Water was purified using a Milli-Q Plus system.6.

Synthesis of Fe_3O_4 Nanoparticles

Iron-oxide nanoparticles were synthesized by the chemical precipitation of Fe^{3+} and Fe^{2+} ions in a 2 : 1 molar ratio from an aqueous solution with the addition of ammonia hydrate [23]. To prevent aggregation, we stabilized the nanoparticles by citrate ions with a negative charge.

Synthesis of Polyelectrolyte Microcapsules

The microcapsules were synthesized using the layer-by-layer adsorption method on calcium-carbonate particles [4]. To obtain calcium-carbonate particles and include dextran labeled with tetramethylrhodamine-5-isothiocyanate (TRITC-dextran) into microcapsules by coprecipitation, 615 μL each of $CaCl_2$ and Na_2CO_3 (1 mol/L) aqueous solutions and 2 mL of the TRITC-dextran (2 mg/mL) solution were taken. The formed crystals of calcium carbonate captured TRITC-dextran, which resulted in its enclosure inside the particles. To adsorb the nanoparticles, 100 μL of an aqueous suspension of nanoparticles (the concentration (~2.3×10^{27} pieces) was calculated from the reaction equation [23]) was added to each test tube, mixed in a shaker for 15 min, and rinsed once. To dissolve calcium-carbonate particles, 1 mL of an aqueous solution of EDTA disodium salt (0.2 mol/L) was added to the sample, mixed in a shaker for 15 min, centrifuged, and the supernatant was removed. The process was repeated three times; the obtained microcapsules were rinsed with deionized water three times. The concentration of microcapsules—~6.9×10^8 pieces—was calculated from the equation of the reaction of calcium-carbonate formation. The composite shell had the following structure: PAH/PSS/PAH/MNP/PSS/PAH/PSS (MNP is magnetic nanoparticle).

Effect of a Low-Frequency Alternating Magnetic Field on Composite Microcapsules

To release TRITC-dextran from polyelectrolyte microcapsules, a TOR MFG 01/12 alternating-magnetic-field generator (Nanomaterials, Russia) was used. The microcapsules were affected by a continuous alternating magnetic field with an amplitude of 100 mT and a frequency of 30–110 Hz. The experiment was carried out on four series of samples at an exposure frequency of 30, 50, 77, and 110 Hz. The microcapsule sample was divided into five pieces (including the reference sample); then, the test tubes with composite microcapsules were placed in the working area of the magnetic-field generator using a special holder. The concentration of microcapsules in each test tube was ~1.4×10^8 pieces; each series of samples was exposed to the magnetic field for 60 min. Each test tube was centrifuged, the supernatant was taken, and the fluorescence intensity was measured using a Cary Eclipse fluorescence spectrophotometer at the fluorescence excitation wavelength of TRITC-dextran 552 nm.

An alternating magnetic field with a frequency of 50 Hz was used to determine the optimal exposure time of the microcapsules. The intensity of TRITC-dextran fluorescence in composite microcapsules was measured 2 h after the effect of the magnetic field using a Leica TCS SPE confocal microscope (Leica Camera AG, Germany).

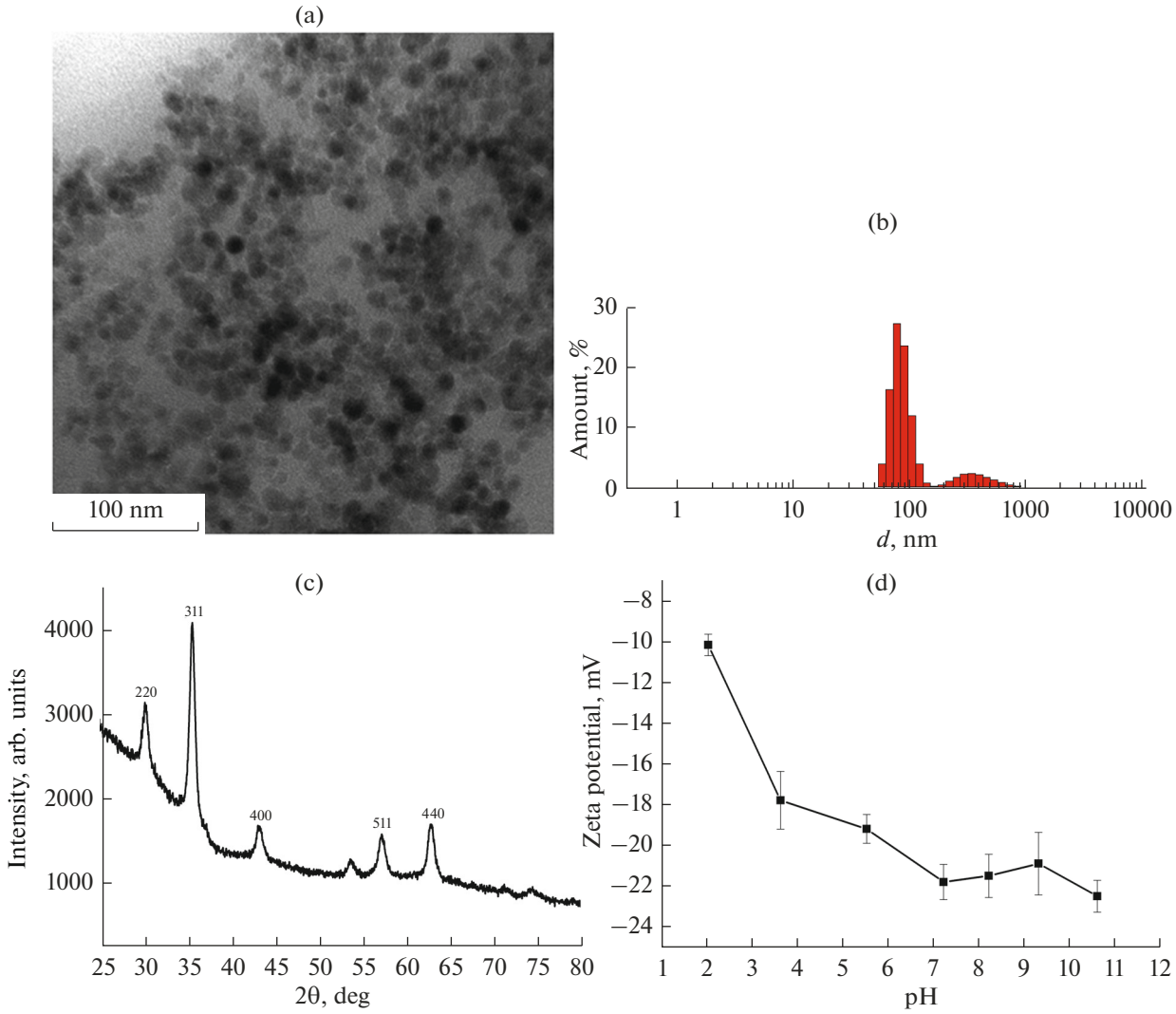

Fig. 1. Magnetic particles Fe_3O_4: (a) TEM image, (b) histogram of the size distribution d, (c) powder XRD pattern, (d) dependence of the zeta potential value on the pH.

RESULTS AND DISCUSSION

A Technai Osiris transmission electron microscope (FEI, USA) and a Malvern Zetasizer ZS analyzer (Malvern Panalytical, United Kingdom) were used to determine the size of the synthesized nanoparticles. Figure 1a presents a TEM image of the synthesized Fe_3O_4 nanoparticles. The shape of the nanoparticles was close to spherical, and their average size was 13 ± 1 nm according to the calculations of the TEM image using ImageJ software. The size distribution of the nanoparticles obtained by dynamic light scattering is given in Fig. 1b, which shows some agglomerates of nanoparticles in the suspension and individual nanoparticles. The hydrodynamic size of Fe_3O_4 nanoparticles is 85 ± 16 nm, which is several times larger than the size obtained by electron microscopy. Such behavior indicates the formation of the adsorption layer of molecules and ions of the environment on the surface of nanoparticles.

The powder X-ray diffraction patterns of the nanoparticles (Fig. 1c) were collected using a Rigaku Miniflex 600 diffractometer (λ = 1.5406 Å). According to the JCPDS database (No. 89-4319), the reflections 220 (2θ = 30.0°), 311 (2θ = 35.2°), 400 (2θ = 42.9°), 511 (2θ = 56.9°), and 440 (2θ = 62.5°) correspond to the cubic crystal structure of the spinel typical for magnetite Fe_3O_4 (space group $Fd\bar{3}m$). The average size of the coherent scattering area (estimated by the Scherrer formula assuming the spherical shape of the nanoparticles with constant $K = 0.9$) was 15 nm, which agrees with the TEM data. The phase composition of the nanoparticles was studied by Mössbauer spectroscopy in the transmission geometry using a γ-radiation source $^{57}Co(Rh)$ and an MS-1104Em spectrometer. Analysis of the Mössbauer spectra indi-

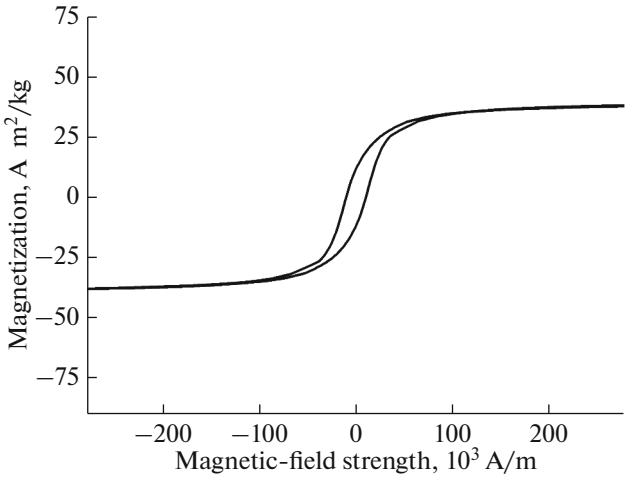

Fig. 2. Magnetization curve of synthesized nanoparticles.

cated the presence of the magnetic phase maghemite γ-Fe_2O_3. The change in the zeta potential of Fe_3O_4 nanoparticles depending on the acidity of the dispersed phase (Fig. 1d) demonstrates an increase in the modulus of the zeta potential as the pH increases from 2 to 7. Because a further increase in pH does not lead to growth of the modulus of the electrokinetic potential, the nanoparticles on the polymer shells were absorbed on a layer of polycation from a suspension of nanoparticles at a neutral pH.

The magnetic properties of the Fe_3O_4 nanoparticles were determined from the hysteresis curve (Fig. 2) obtained using an EG&G PARC vibrating sample magnetometer (model 155). The coercive force was 1.06 ± 0.01 kA/m, the specific saturation magnetization was 38.7 A m^2/kg, and the magnetic moment was $(2.4 \pm 0.3) \times 10^{-19}$ A m^2. The hysteresis curve observed at room temperature indicates that the Fe_3O_4 nanoparticles have a ferromagnetic nature. According to existing ideas, the synthesized nanoparticles are single-domain and can relax by the Brownian mechanism in a low-frequency alternating magnetic field; they can be used as mediators of local deformation due to magnetomechanical activation [20]. For its implementation, the parameters of the nanoparticle (diameter, material) and the magnetic field (amplitude-frequency and space-time characteristics) are important. Efficient magnetochemical activation requires low-frequency alternating magnetic fields (less than 0.1–1 kHz) and a diameter of magnetic nanoparticles from 15 to 100 nm because the nanoparticles should remain single-domain (magnetite transforms to a multidomain state at a diameter of about 100 nm) and an increase in the size of the nanoparticles enhances the maximum generated force in an alternating magnetic field due to growth of the magnetic moment [24]. Thus, the field and particles used are suitable for mechanochemical activation. Complex association of the effect value (deformation) with the field frequency dependent on the surrounding of the nanoparticles is typical for mechanochemical activation. Macromolecules connected with nanoparticles can have inverse relaxation times lying in the region of low frequencies of alternating magnetic fields, which leads to pseudo-resonance effects of increasing the response [24, 25].

As is seen in Fig. 3a (the image of microcapsules obtained using a fluorescence confocal microscope) TRITC-dextran is successfully included into $CaCO_3$ particles during coprecipitation. The average hydrodynamic diameter of the synthesized microcapsules determined by dynamic light scattering was 3.7 ± 0.5 μm. To study the effect of a low-frequency alternating magnetic field on the shell morphology, microcapsules were treated by a field with an amplitude of 100 mT and frequencies of 30, 50, 77, and 110 Hz. A JSM-7401F scanning electron microscope (Jeol, Japan) was used to study the violation of the integrity of the shell of the polyelectrolyte microcapsule; the

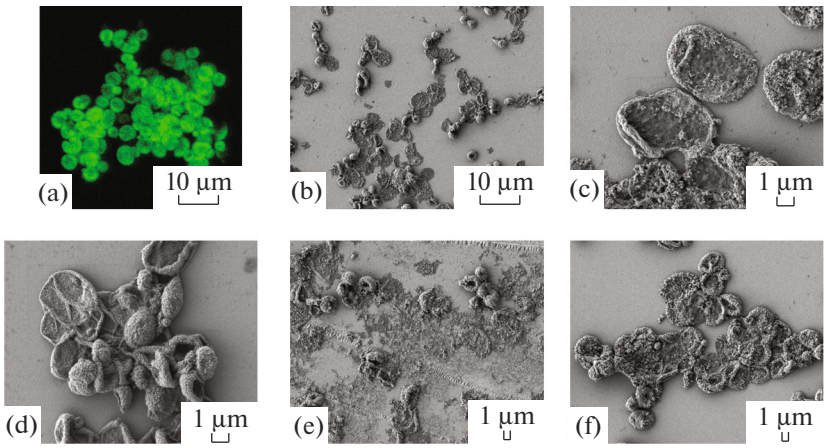

Fig. 3. Images of microcapsules obtained by fluorescence confocal microscopy (a) and SEM (b – f) before (a, b) and after (c–f) impact of the alternating magnetic field with the amplitude of 100 mT for 60 min with the frequency: (c) 30, (d) 50, (e) 77, and (f) 110 Hz.

SEM images presented in Figs. 3b–3f were used to consider the violation.

When no field is applied, the shell is undisturbed, and the microcapsules are unbroken (Fig. 3b). Comparing the images, we can see that the largest deformation is observed under the effect of an alternating magnetic field with a frequency of 77 Hz (Fig. 3d). No visible deformations are observed at frequencies of 30, 50, and 110 Hz (Figs. 3c, 3e, and 3f). The main cause of the visible breaking of microcapsules can be pseudo-resonance in the "shell–nanoparticles" system when the reciprocal relaxation time of the multilayer polyelectrolyte shell coincides with the frequency of the magnetic field. With Brownian relaxation under the effect of a low-frequency alternating magnetic field, magnetic nanoparticles start to oscillate. Their mechanical energy passes to the shell as compression and tension deformations of macromolecules constituting composite microcapsules; at a frequency of 77 Hz, these deformations increase many times, i.e., they are resonant. Under such an effect, encapsulated TRITC-dextran is released from the microcapsules.

Table 1 lists the intensity of TRITC-dextran fluorescence in the supernatant after the influence of an alternating magnetic field with different frequencies on the microcapsules; each measurement was conducted 2 h after the action. It is seen that TRITC-dextran releases in all cases. As for the reference sample (without the action), the release is connected with the diffusion of TRITC-dextran from the microcapsule to the supernatant, and it is minimal compared with the other samples. Microcapsule shells are practically impermeable to compounds with a molecular weight greater than 5 kDa [9]. Therefore, we can suppose that the change in the fluorescence due to natural diffusion is not statistically significant in this time interval. The maximum intensity of supernatant fluorescence is observed at a field frequency of 77 Hz, which agrees with the SEM result.

The time of exposure of microcapsules in the low-frequency magnetic field is one of the impact parameters. Using confocal microscopy, we obtained data on the intensity of TRITC-dextran fluorescence in microcapsules depending on the time of exposure to a magnetic field (Fig. 4). When the exposure time exceeds 10 min, the intensity of TRITC-dextran fluorescence is almost unchanged, which indicates the establishment of an equilibrium concentration in the shell and dispersed medium and the end of the release process. Thus, the optimal time of field impact is 10 min: during this time, an equilibrium concentration of TRITC-dextran is established in the membrane and in the medium in which the microcapsules are located.

Table 1. Intensity of TRITC-dextran fluorescence in the supernatant after the impact of an alternating magnetic field of different frequencies and centrifugation of microcapsules

Impact frequency, Hz	Fluorescence intensity, arb. units
0	21.8
30	42.1
50	40.9
77	84.4
110	71.6

CONCLUSIONS

We demonstrated the successful application of a low-frequency alternating magnetic field for the controlled release of TRITC-dextran from composite microcapsules. According to analysis of the obtained results, the system of the multilayer polyelectrolyte shell that contains magnetite nanoparticles has a definite inverse relaxation time close to 77 Hz. When PAH/PSS/PAH/MNP/PSS/PAH/PSS composite capsules are placed in a magnetic field with a frequency of 77 Hz, a pseudo-resonance appears that causes shell defects and stimulates the release of the encapsulated substance. The optimal time of magnetic-field action is 10 min.

Magnetomechanical activation is the basis for a new concept of local action at the molecular level. It is promising for controlling the permeability of micro-

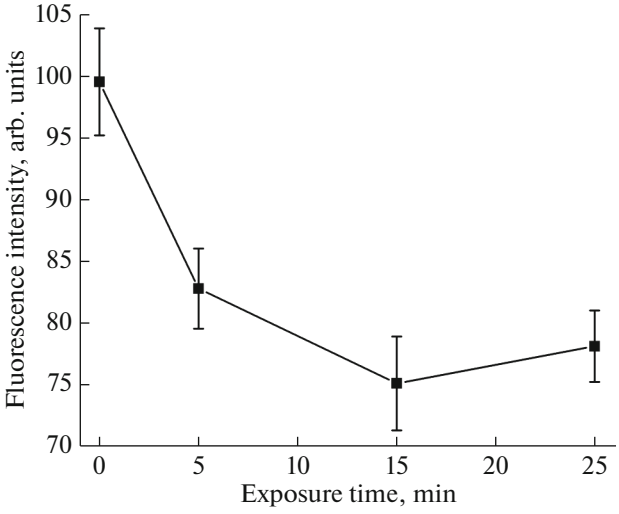

Fig. 4. Dependence of the fluorescence intensity of TRITC-dextran in the shell of microcapsules on the exposure time in a magnetic field with an amplitude of 100 mT and a frequency of 50 Hz.

capsule shells during the delivery of biologically active substances.

ACKNOWLEDGMENTS

The study was performed using the equipment of the Center for Collective Use of the Federal Research Center "Crystallography and Photonics," Russian Academy of Sciences.

FUNDING

This work was carried out within the framework of the state assignment of the Federal Research Center "Crystallography and Photonics," Russian Academy of Sciences. It was supported by the RF Ministry of Science and Higher Education (project RFMEFI62119X0035) in terms of the synthesis and characterization of iron-oxide nanoparticles. The work on modifying the capsule shells with iron-oxide nanoparticles and analyzing the effect of a non-heating magnetic field was supported by the Council for Grants of the President of the Russian Federation (no. MK-1109.2021.1.3).

CONFLICT OF INTEREST

The authors declare that they have no conflict of interest.

REFERENCES

1. N. Dimov, E. Kastner, M. Hussain, and Y. Perrie, N. Szita, Sci. Rep. **7**, 12045 (2017).
2. Y. Zhang, Y. Huang, and S. Li, AAPS PharmSciTec **15**, 862 (2014).
3. O. M. Elsharkasy, J. Z. Nordin, D. W. Hagey, O. G. de Jong, R. M. Schiffelers, S. El Andaloussi, and P. Vader, Adv. Drug Delivery Rev. **159**, 332 (2020).
4. E. Donath, G. B. Sukhorukov, F. Caruso, S. A. Davis, and H. Möhwald, Angew. Chem., Int. Ed. **37**, 2201 (1998). https://doi.org/10.1002/(SICI)1521-3773(19980904)37:16<2201::AID-ANIE2201>3.0.CO;2-E
5. E. Kilic, M. V. Novoselova, S. H. Lim, N. A. Pyataev, S. I. Pinayev, O. A. Kulikov, O. A. Sindeeva, O. A. Mayorova, R. Murney, M. N. Antipina, B. Haigh, G. B. Sukhorukov, and M. V. Kiryukhin, Sci. Rep. **7**, 44159 (2017).
6. B. G. de Geest, M. A. Willart, H. Hammad, B. N. Lambrecht, C. Pollard, P. Bogaert, M. de Filette, X. Saelens, C. Vervaet, J. P. Remon, J. Grooten, and S. de Koker, ACS Nano **6**, 2136 (2012). https://doi.org/10.1021/nn205099c
7. A. N. Somov, A. V. Dubrovskii, I. A. Dunaitsev, S. A. Ivanov, T. I. Kombarova, O. Yu. Kochetkova, T. B. Kravchenko, G. M. Titareva, S. A. Tikhonenko, A. S. Pinchuk, V. V. Firstova, and S. V. Dentovskaya, Immunologiya **40** (5), 52 (2019. https://doi.org/10.24411/0206-4952-2019-15006
8. O. E. Selina, S. Yu. Belov, N. N. Vlasova, V. I. Balysheva, A. I. Churin, A. Bartkoviak, G. B. Sukhorukov, and E. A. Markvicheva, Russ. J. Bioorg. Chem. **35**, 103 (2009). https://doi.org/10.1134/S1068162009010130
9. L. J. de Cock, S. de Koker, B. G. de Geest, J. Grooten, C. Vervaet, J. P. Remon, G. B. Sukhorukov, and M. N. Antipina, Angew. Chem., Int. Ed. **49**, 6954 (2010).
10. Z. She, M. N. Antipina, J. Li, and G. B. Sukhorukov, Biomacromolecules **11**, 1241 (2010).
11. T. Borodina, E. Markvicheva, S. Kunizhev, H. Mohwald, G. B. Sukhorukov, and O. Kreft, Macromol. Rapid Commun. **28**, 1894 (2007).
12. B. G. de Geest, A. G. Skirtach, A. A. Mamedov, A. A. Antipov, N. A. Kotov, S. C. de Smedt, and G. B. Sukhorukov, Small **3**, 804 (2007).
13. A. V. Petrov, D. V. Voronin, O. A. Inozemtseva, V. V. Petrov, and D. A. Gorin, Vestn. Tambov. Gos. Tekh. Univ. **24**, 539 (2018). https://doi.org/10.17277/vestnik.2018.03.pp.539-549
14. T. Borodina, D. Yurina, A. Sokovikov, D. Karimov, T. Bukreeva, E. Khaydukov, and D. Shchukin, Polymer **212**, 123299 (2020).
15. I. V. Marchenko, G. S. Plotnikov, A. N. Baranov, A. M. Saletskii, and T. V. Bukreeva, J. Surface Invest.: X-ray, Synchrotron Neutron Tech. **4**, 95 (2010).
16. I. V. Marchenko, T. N. Borodina, D. B. Trushina, B. V. Nabatov, V. V. Logachev, G. S. Plotnikov, A. N. Baranov, A. M. Saletskii, A. V. Ryabova, and T. V. Bukreeva, Colloid J. **80**, 399 (2018). https://doi.org/10.1134/S1061933X18040075
17. Z. Lu, M. D. Prouty, Z. Guo, V. O. Golub, C. S. S. R. Kumar, and Y. M. Lvov, Langmuir **21**, 2042 (2005).
18. S. Carregal-Romero, P. Guardia, X. Yu, P. Hartmann, T. Pellegrino, and W. J. Parak, Nanoscale **7**, 570 (2015).
19. S.-H. Hu, C.-H. Tsai, C.-F. Liao, D.-M. Liu, and S.-Y. Chen, Langmuir **24**, 11811 (2008). : https://doi.org/10.1021/la801138e
20. Y. I. Golovin, N. L. Klyachko, A. G. Majouga, S. L. Gribanovskii, D. Y. Golovin, A. O. Zhigachev, A. V. Shuklinov, M. V. Efremova, M. M. Veselov, K. Y. Vlasova, A. D. Usvaliev, I. M. Le-Deygen, and A. V. Kabanov, Nanotechnol. Russ. **13**, 215 (2018).
21. P. V. Finotelli, D. D. Silva, M. Sola-Penna, A. M. Rossi, M. Farina, L. R. Andrade, A. Y. Takeuchi, and M. H. Rocha-Leão, Colloids Surf., B **81**, 206 (2010).
22. D. Luo, R. N. Poston, D. J. Gould, and G. B. Sukhorukov, Mater. Sci. Eng., C **94**, 647 (2019).
23. R. Massart, IEEE Trans. Magn. **17**, 1247 (1981).
24. Y. I. Golovin, M. V. Zhigachev, M. V. Efremova, A. G. Majouga, A. V. Kabanov, and N. L. Klyachko, Nanotechnol. Russ. **13**, 295 (2018).
25. M. V. Efremova, M. M. Veselov, A. V. Barulin, et al., ACS Nano **12**, 3190 (2018).

Translated by N. Saetova